J Fluoresc (2010) 20:215–223
DOI 10.1007/s10895-009-0541-4

ORIGINAL PAPER

Optical Properties of Micro-patterned Silver Nanoparticle Substrates

Ondrej Stranik · Daniela Iacopino · Robert Nooney · Colette McDonagh · Brian D. MacCraith

Received: 9 June 2009 / Accepted: 15 September 2009 / Published online: 10 October 2009

Abstract In this paper, we describe a novel technique for depositing metal nanoparticles (NPs) on a planar substrate whereby the NPs are micro-patterned on the surface by a simple stamp-printing procedure. The method exploits the attractive force between negatively charged colloidal metal NPs and positively-charged polyelectrolyte layers which have been selectively deposited on the surface. Using this technique, large uniform areas of patterned metal NPs, with different plasmonic properties, were achieved by optimisation of the stamping process. We report the observation of unusual fluorescence emission from these structures. The emission was measured using epifluorescence microscopy. Fluorescence lifetime behaviour was also measured. Furthermore, the μ-patterned NPs exhibited blinking behaviour under 469 nm excitation and the fluorescence spectrum was multi-peaked. It has been established that the fluorescence is independent of the plasmon resonance properties of the NPs. As well as optimising the novel NP μ-patterning technique, this work discusses the origin and characteristics of the anomalous fluorescence behaviour in order to characterise and minimise this unwanted background contribution in the use of metal NPs for plasmonic enhancement of fluorescence for optical biochip applications.

Keywords Metal nanoparticles · Stamp-printing · Fluorescence · Plasmonics

Electronic supplementary material The online version of this article (doi:10.1007/s10895-009-0541-4) contains supplementary material, which is available to authorized users.

O. Stranik · R. Nooney · C. McDonagh (✉) · B. D. MacCraith
Biomedical Diagnostics Institute, School of Physical Sciences,
Dublin City University,
Glasnevin,
Dublin 9, Ireland
e-mail: Colette.mcdonagh@dcu.ie

D. Iacopino
Nanotechnology Group, Tyndall Institute, Lee Maltings,
University College,
Cork, Ireland

Introduction

Metal nanostructures are of significant interest because they can confine light into the sub-wavelength area at their interfaces and this strongly localised light can be used in a variety of optical and sensing applications [1]. A special subclass of these structures are metal nanoparticles (NPs), typically made from silver and gold, the noble metals. These nanoparticles exhibit strong absorption of visible light, which arises from the localised surface plasmon resonance (LSPR) properties of the NPs [2]. LSPR is strongly dependent on several parameters such as NP size, shape and composition. This gives rise to many useful applications for metal NPs, particularly in the area of biosensing. [3–6]. NPs are used to enhance optical processes such as Raman, fluorescence or scattering [7–10]. In recent years, there has been much published work in the area of plasmonic enhancement of fluorescence. For optical biochip applications, it is relevant to examine the enhancement behaviour in planar experimental configurations where monolayers of NPs and fluorescent dye labels are deposited.

The preparation of large numbers of monodispersed metal NPs is still a challenging issue. Using wet chemistry, the size and the shape can be partially controlled and the resulting NPs form a colloidal suspension. In this process,

the metal ions undergo chemical reduction in the presence of stabilizing agents [11]. In another technique, NPs are formed on a substrate using templating/metal deposition. Several methods such as e-beam lithography, dip-pen lithography, nanosphere lithography [12–14] are currently used. In general, these techniques have good nanostructure resolution and reproducibility, but suffer from low throughput and high equipment cost. Previous work in this laboratory has established a reproducible technique for depositing NPs on charged polyelectrolyte layers on a planar substrate and substantial plasmonic enhancement has been demonstrated for a model assay [15].

Here, we report on the development of a simpler technique which also yields reproducible NP layers. Firstly, silver nanoparticles of different sizes were synthesized by reducing silver nitrate with sodium citrate in the presence of aniline. NPs were then patterned onto a substrate using a stamp-printing method. The process of selective deposition of metal NPs onto a surface uses polyelectrolytes (PELs), which are water-soluble charged polymers. They are either positively or negatively charged and are able to form nm-thin uniform layers based on electrostatic interaction. [16, 17]. Moreover, PEL layers can be selectively transferred onto a surface using a stamp-printing method [18, 19].

As well as the development and characterisation of the novel NP stamp-printing technique, we also characterised the intrinsic fluorescence and blinking behaviour of the NPs. This effect has not been widely observed and we propose some mechanisms in order to explain the phenomenon.

The motivation for this work is two-fold: (i) to develop a facile and reproducible method of metal NP deposition on planar substrates for optical biochip applications and (ii) to elucidate the intrinsic NP fluorescence and blinking behaviour in order to minimise the NP background in plasmonic enhancement measurements.

Experimental

Synthesis of silver nanoparticles

NPs of 60 nm±10 nm in diameter were prepared by reducing silver nitrate with sodium citrate in the presence of aniline [20]. Briefly, 4 ml of $AgNO_3$ (0·02 M) and 4 mL of aniline (0·02 M) were dissolved in 104 mL of deionised water (dH_2O) and purged with nitrogen. The solution was heated to boiling and 8 mL of 1 wt % sodium citrate added with rapid stirring. The solution was refluxed for 30 min during which time the solution changed color from clear to dark brown. The solution was centrifuged at 13,000 rpm for 5 min and doubly concentrated in deionised water. The colloid was stored in a polystyrene bottle at 4 °C. The final concentration of colloid was estimated to be $1{\cdot}6\times10^{13}$ particles per mL and the suspension exhibited a plasmon absorption peak at 425 nm (see Fig. 3). Larger NPs (149± 16 nm) were prepared under the same conditions without stirring.

Fabrication of NP-patterned substrates

Standard glass microscope cover slips (Menzel Glaser) were used as substrates. Prior to the PEL layer attachment the slips were cleaned by 15 min sonication in a solution of 1% wt KOH in ethanol/water (3:2), 15 min sonication in dH_2O, dried under stream of N_2. The slides were then exposed to air plasma in a plasma chamber (Harrick) for 5 min to create a charged surface. Our protocol for creating PEL stamp printed patterns was based on the method described in reference [21] and was optimized for our application (see later). The multilayers of PEL were constructed on cover slips in the following way. The slides were immersed for 5 min in a solution of 0.05 M (based on polymer repeat unit) poly(diallyldimethylammonium chloride) of 400,000 molecular weight (PDAC) and 0.1 M NaCl. After cleaning with deionised H_20 the slides were immersed for 5 min in a solution of 0.05 M (based on polymer repeat unit) poly(sodium 4-styrene sulfonate) of 70,000 molecular weight (PSS) and 0.1 M NaCl and again rinsed with dH_2O. These two immersions were repeated to form at the surface a uniform layer of negatively charged PEL. This stage in the process is shown schematically in Fig. 1a.

Stamps for selective transfer of PEL were made from Poly(dimethylsiloxane) (PDMS) using a "two-ingredient" elastomer kit Sylguard 184. The PDMS was cured on top of a silicon master, which has parallel lines 10μm wide, 10 μm high with 10 μm spacing. The resultant stamp was exposed to air plasma in a plasma chamber (Harrick) for 5 min to render the surface hydrophilic. Then it was immersed in a solution of 0.25 M PDAC of 400,000 molecular weight in ethanol/water (1:1) for 5 min. The stamp was washed with dH_2O and dried with a stream of N_2 (Fig. 1b). The stamp was applied to a cover slip with PEL layers. After 1 h of contact, the stamp was removed and the substrate was washed with H_2O and dried with N_2 (Fig. 1c) In the final stage, the cover slip was immersed in a solution of NPs and left to incubate for 1 h, followed by washing with H_2O and drying with N_2 (Fig. 1d).

Widefield microscopy

Prepared solutions of NPs were diluted with dH_2O in a cuvette and their absorption spectra were measured using a uv-vis spectrometer (Tecan, Inc). The transmission

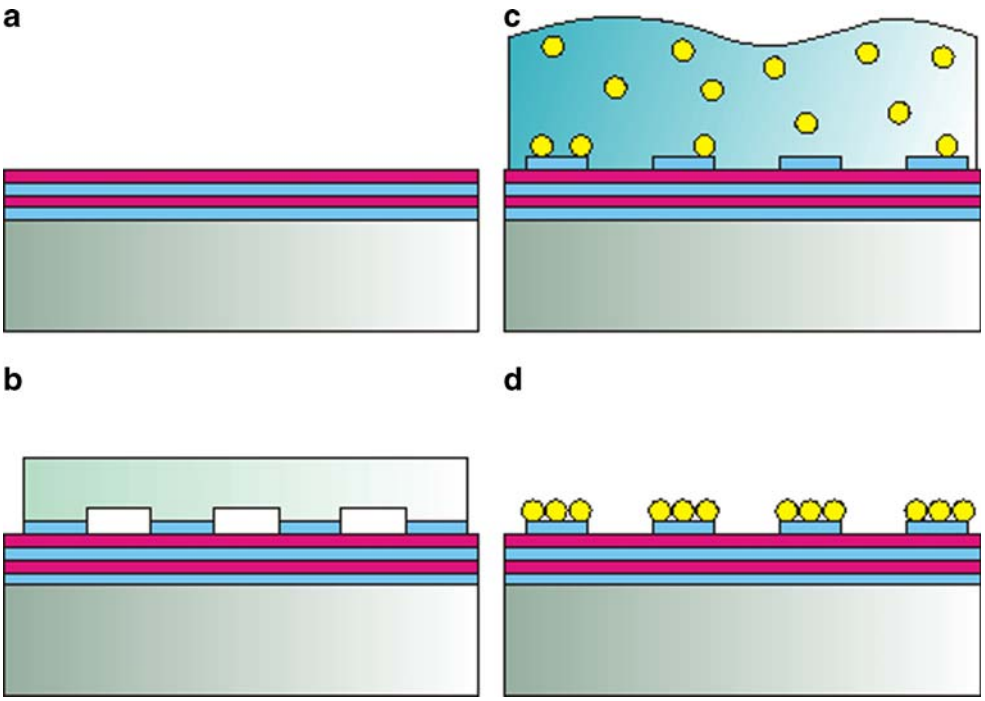

Fig. 1 Steps in preparation of metal nanoparticles μ-patterned structures. **a** formation of PEL layers **b** stamp-printing of positively charged PEL **c** electrostatic adsorption of NPs **d** washing of unbound NPs

images of samples with micro patterned NPs were recorded on an inverted microscope (Olympus IX 71). The fluorescence images were recorded using an epifluorescence inverted microscope (Olympus IX 71) equipped with a CCD camera (F-view II, Olympus). The filter cube included an excitation filter 447/60 nm, dichroic 510 nm and emission filter 625/26 nm (Semrock). The recorded sequence of fluorescence images had exposure time 200 μs.

Fluorescence lifetime imaging

Fluorescence lifetime measurements were carried out on a scanning confocal fluorescence microscope (MicroTime 200, PicoQuant GmbH.) equipped with a XY piezoelectric scanning stage (P-733-2CL, Physik Instrumente GmbH.). System operation was controlled by a dedicated software package (SymPhoTime 4.7 software, PicoQuant GmbH.). The output of a 469 nm pulsed picosecond laser diode (20 Mhz; 70 ps pulse direction; LDH-P-C-470, PicoQuant GmbH) was coupled into the main confocal unit using a polarization maintaining single mode optical fiber, collimated, and spectrally filtered using a 467 nm band pass filter (z467/10X, Chroma Technology Corp.). The horizontally polarized laser light was then converted to circularly polarized light using a wedge polariser (WDPOL, Thorlabs Inc.). The collimated laser beam was then directed into the entrance port of an inverted

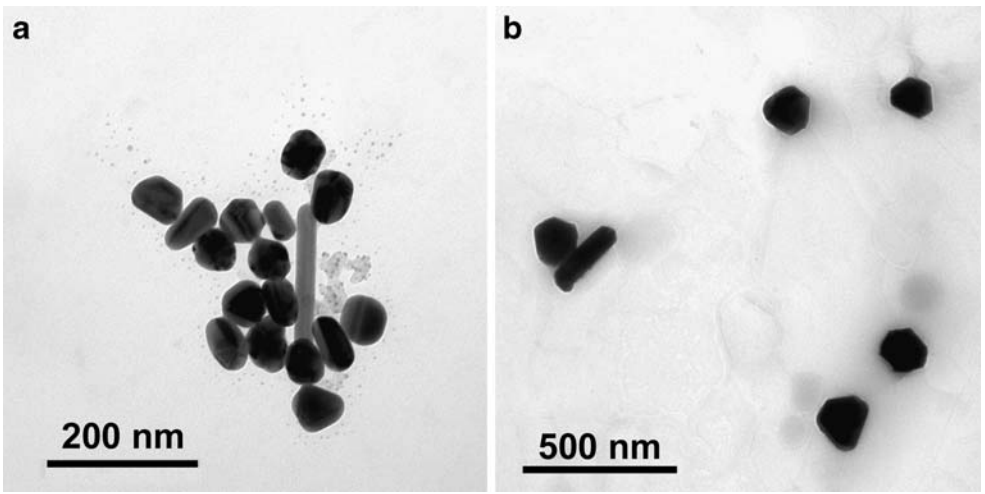

Fig. 2 TEM images of synthesized metal nanoparticles **a** small NPs 60±10 nm in size **b** large NPs 149±16 nm in size

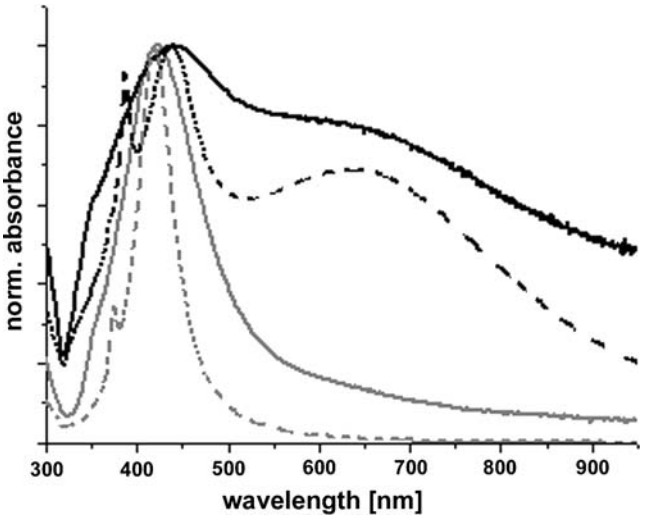

Fig. 3 Absorption spectra of 149 nm (*black*) and 60 nm (*grey*) nanoparticles (*dashed lines* are theoretical fits)

microscope (IX 71, Olympus Corp.) using a dichroic mirror (480dcxr, Chroma Technology Corp.) and directed onto the sample using 100X oil immersion objective (1.4 NA, UPlan SAPO, Olympus). Fluorescence was collected by the same objective, passed through the dichroic mirror, spatially filtered by focusing onto a 50 mm diameter pinhole to reject out-of-focus signals, re-collimated, and directed onto an avalanche photodiode (APD; SPCM-AQR-14, Perkin-Elmer Inc.). Back-scattered excitation light was blocked with a 500 nm long-pass filter placed in the collection path (HQ500LP, Chroma Technology Corp.).

Scanning confocal emission images were recorded by raster scanning the sample through the laser focus spot and recording the resulting fluorescence at the APD. Following image acquisition, fluorescence lifetime transients were recorded using a time correlated single photon counting (TCSPC) technique with a TimeHarp 200 board (PicoQuant GmbH). The excitation power was adjusted to maintain a count rate of $<10^4$ counts/s at the APD in order to preserve single photon counting statistics. All emission lifetimes were fitted with a multi-exponential and experimentally measured instrumental response function reconvolution model using FluoFit 4.2 software (PicoQuant GmbH).

Emission spectra were recorded by directing the photoluminescence onto the entrance slit of a 0.3 m monochromator (SP-2356, 300 g/mm grating, 500 nm blaze, Acton Research) equipped with a thermoelectrically cooled, back illuminated CCD (Spec10:100B, Princeton Instruments). Spectra were recorded using an integration time of 60 s and a slit width of 500 μm.

Results and discussion

NP characterisation and spectral properties

Solutions of silver nanoparticles of two different sizes were synthesised. The TEM images of the colloids are shown in Fig. 2. The shapes of the NPs are in both cases quasi-spherical with average diameter 60 nm±10 nm for smaller NP (Fig. 2a) and 149±16 nm for large NPs (Fig. 2b). These diameters were determined from TEM measurements. These NPs exhibit characteristic absorption caused by LSPR. Their normalised absorption spectra are presented in Fig. 3. The spectrum of the smaller NPs consists of a single peak centred at 420 nm with small peak at 354 nm. The spectrum of the larger NPs consists of the superposition of a main peak at 440 nm and additional peaks at 650 nm and 350 nm. The spectra in Fig. 3 were overlapped with a theoretical fit (dashed line) based on Mie theory [22]. From the simulation we measured the diameters of the NPs to be 68 nm and 160 nm for the smaller and the larger NPs respectively which agrees well with the experimentally measured values within the measurement error. The multi-peaked spectrum for the larger NPs is caused by higher order multi-pole LSPR excitation.

μ-patterning of NPs

The colloidal silver NPs were selectively attached onto substrates using the method described earlier. The procedure was optimised to achieve high NP surface coverage. Two key optimisation steps were: (i) washing the stamp with dH_2O after incubation with inking PEL solution and drying with N_2. This step left only an ultra thin layer of PEL on the stamp and PEL on the protruded part of the stamp was then transferred onto a cover slip achieving high resolution of the patterning and (ii) leaving the stamp in

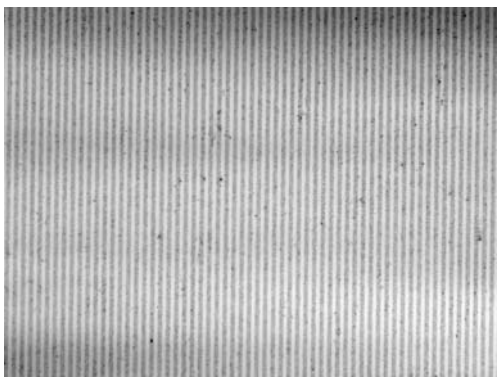

Fig. 4 Transmission image of metal nanoparticle patterned structures. The width of the lines is 10 μm and spacing is 10 μm

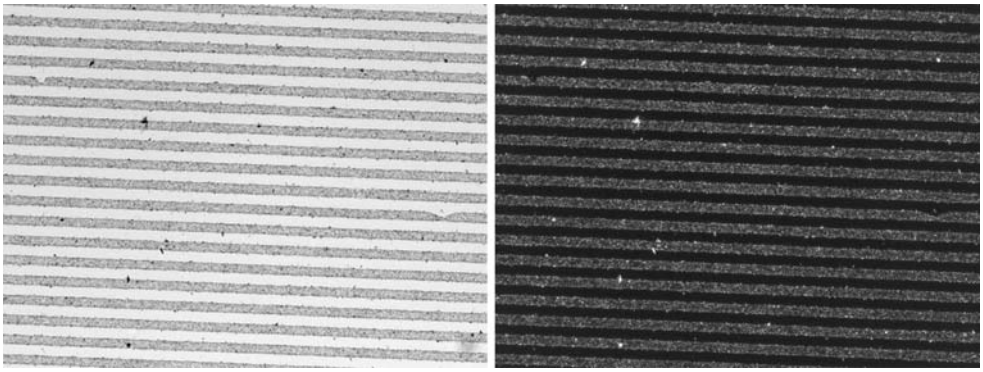

Fig. 5 Contrast (*left*) and fluorescence (*right*) image of 149 nm size metal nanoparticle patterned structures

contact with a cover slip for a sufficiently long time (generally 1 h) allowing complete transfer of the inking PEL on a substrate.

In our samples, patterns of 10 μm wide and 10 μm-spaced lines were used, and both types of NPs were used for the attachment. In both cases, we were able to reproduce the patterns almost over the whole stamp area (0.5 cm× 0.5 cm) with high NP coverage and high NP contrast between the patterned and non-patterned area. Figure 4 shows a transmission image of a patterned substrate with 60 nm silver NPs.

Fluorescence response of μ-patterned NPs

The fluorescence properties were investigated using a range of techniques including wide field microscopy, time-correlated single photon counting and lifetime measurements. The samples were excited at 449 nm (central wavelength) and the emission was collected at 625 nm (central wavelength). Under such conditions, fluorescence from samples with both types of silver NPs was observed. An example of the transmission (left) and fluorescence (right) of a μ-patterned sample with 149 nm diameter silver NPs is shown in Fig. 5. The patterns are identical in both cases indicating that the fluorescence is originating from the NPs. The striking observation was that the fluorescence exhibits blinking behaviour. The duration of the blinking was variable ranging from sub-second range up to several seconds, and the ratio of on-state and off-state varied also. A sequence of images recording this blinking fluorescence behaviour is shown in Movie 1 (Supplementary information). Because the speed of recording was limited to 3 frame per seconds, a blinking frequency higher ~3 Hz is not distinguishable.

An attempt was made to measure the fluorescence from a pure solution of NPs using a standard spectrofluorometer. However, we did not resolve any fluorescence signal from either types of NPs and the measurement curves just exhibited a strong background signal caused by high scattering efficiency of the NPs.

The fluorescence was further investigated by a time correlated single photon counting technique on a scanning laser confocal microscope. This allowed us to obtain information about the fluorescence lifetime of the silver NPs. The fluorescence was excited with a 469 nm laser line and the emission was collected above 500 nm. The fluorescence intensity images from samples with patterned 60 nm (right) and 149 nm (left) silver NPs are shown in Fig. 6. The fluorescence intensity is not homogenous, with some areas being much brighter than others (Fig. 7).

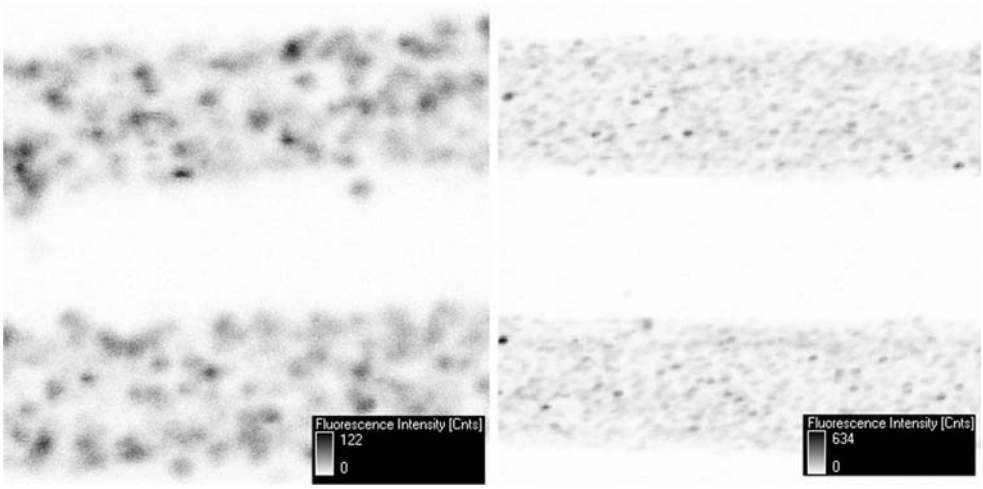

Fig. 6 Fluorescence intensity image (FLIM system) of metal (*left*—149 nm size, *right*—60 nm) nanoparticles patterned structures

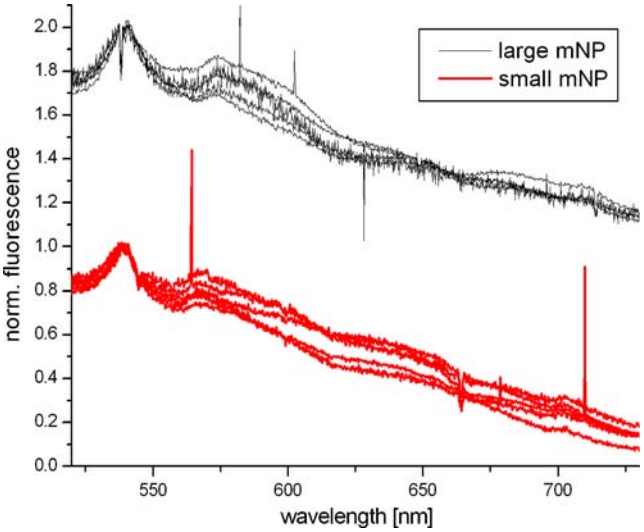

Fig. 7 Fluorescence emission spectra from metal nanoparticles. *Black offset curves*—from five different spots on a substrate with 149 nm size NPs. *Red curves*—from five different spots on a substrate with 60 nm size NPs

Histograms of the photon emission can be constructed from the measurements and the data are presented in Fig. 8. In order to obtain the fluorescence lifetime, the data were fitted to a double exponential decay (solid lines) together with the instrument response function to account for the finite duration of the laser pulse. The fitted average fluorescence lifetime was 0.26 ns and 0.16 ns for the 60 nm and 149 nm silver NPs respectively. The fitted two exponential decay times are summarized in Table 1. These

Table 1 Table summarising values of fluorescence life times in two exponential decay fits and their weighted average presented in Fig. 8 and 10

	τ_1	τ_2	τ_{avg}
60 nm NPs	0.227 ns	2.113 ns	0.26 ns
149 nm NPs	0.036 ns	2.392 ns	0.16 ns
High emission 69 nm NP	0.192 ns	2.117 ns	0.22 ns
Low emission 69 nm NP	0.203 ns	2.001 ns	0.31 ns

fluorescence lifetimes represent the average from many NPs in both states of high emission intensity and low emission intensity.

We also investigated if there is a difference in the fluorescence lifetime of a NP for the case of high emission and low emission intensities. The blinking behaviour of fluorescence was recorded by fluorescence time tracing from a single spot. In this case the data are binned into 100 ms segment and each segment is plotted against the time axis. Due to the unpredictability of the blinking behaviour, several time traces were taken until a clear signal with blinking behaviour was recorded. The recorded blinking behaviour of a 60 nm silver NP is presented in Fig. 9. The fluorescence was increased several fold for the high emission state. The emission fluctuates at the high emission rate as indicated in the circled area in the figure. Due to the high photon counts in the measurement, it was possible to extract the fluorescence lifetimes of the NPs in both emission states. The fluorescence decays, together

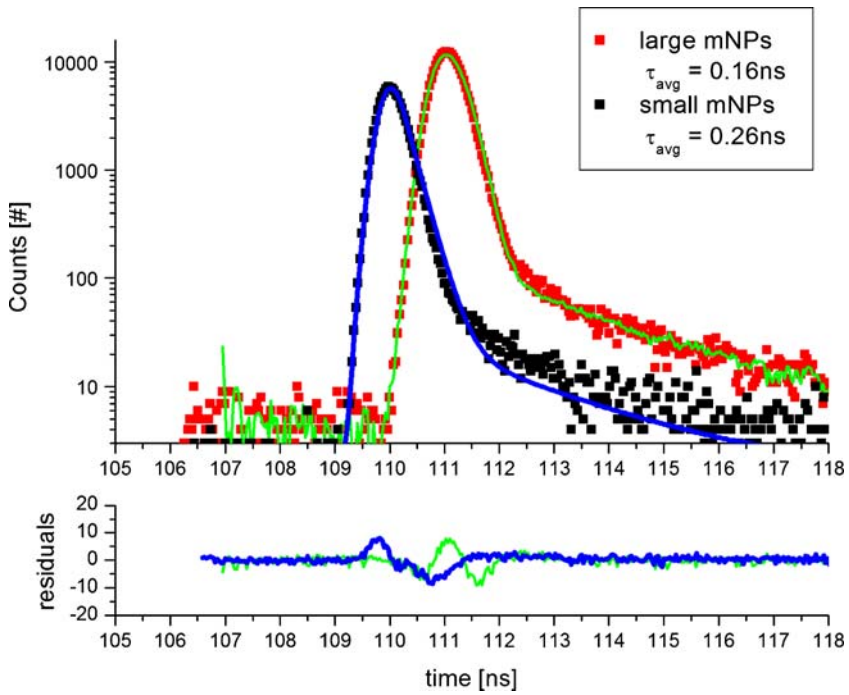

Fig. 8 Fluorescence decays from an ensemble of metal (*black dots*—60 nm size, *red dots*—149 nm size) nanoparticles at states of high and low fluorescence emission. *Solid lines* represent two exponential decay fits with values shown in Table 1. Residual distributions are presented at the bottom graph

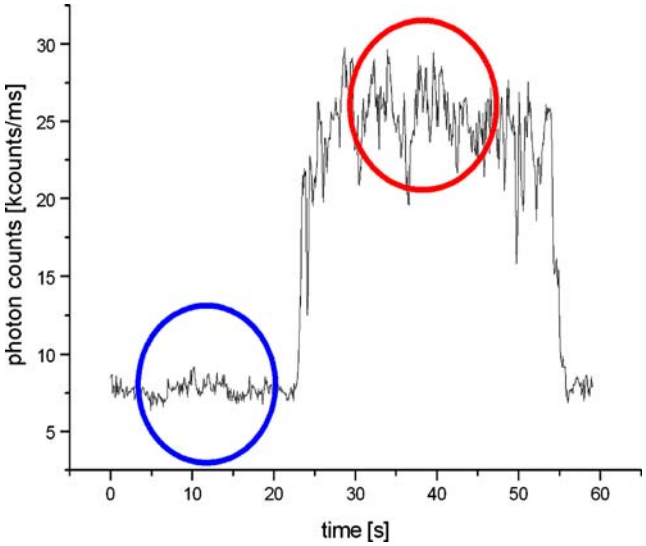

Fig. 9 Fluorescence time trace from 60 nm size nanoparticle. The *circles* represents area of high and low emission state, which were used in analysis in Fig. 10

with their fits (double exponential) are shown in Fig. 10. The average decay is 0.22 ns and 0.31 ns for NP in the higher and lower emission state respectively. The fitted two exponential decay times are summarized in Table 1.

The fluorescence emission spectra from samples were also measured when illuminated by 469 nm. Fluorescence spectra from several spots on the surface with NP-coverage were measured for each NP type. As referred to previously, the normalised emission spectra are presented in Fig. 7. The emission spectra taken from different areas of the same sample are similar in profile. Also, the emission spectra from different NPs do not differ substantially. The spectra consist of four emission peaks at 538 nm, 566 nm, 647 nm and 703 nm from an averaged spectrum. Multicolour blinking has been observed by Geddes et al also for silver nanostructures [23].

Proposed mechanisms for NP fluorescence

The fluorescence behaviour of the patterned NPs can be summarised as being independent of the NP plasmonic properties, having an absorption of ~450 nm, and having multi-peaked emission with sub-ns lifetime. The fluorescence also exhibits a blinking behaviour. Generally, unlike molecular fluorescence, where photon emission is caused by an electron transition between discrete energetic levels [24], bulk metals are almost non-fluorescent, because the electrons in the bulk metal have continuous energy levels and de-excite through thermal processes. Only a very weak fluorescence from metals has been measured with quantum efficiency as low as 10^{-10} [25]. The emission process is explained by de-excitation of conducting electrons in s-p bands with a hole in d-bands of lower energy. An increase of fluorescence from a metal has been observed as a result of roughening the metal surface [26]. This effect was explained by local field enhancement on rough surface protrusions.

However, completely different fluorescent behaviour is observed for an agglomeration of a small number of metal atoms. These clusters form artificial atoms with discrete levels and the fluorescence arises from intraband transitions

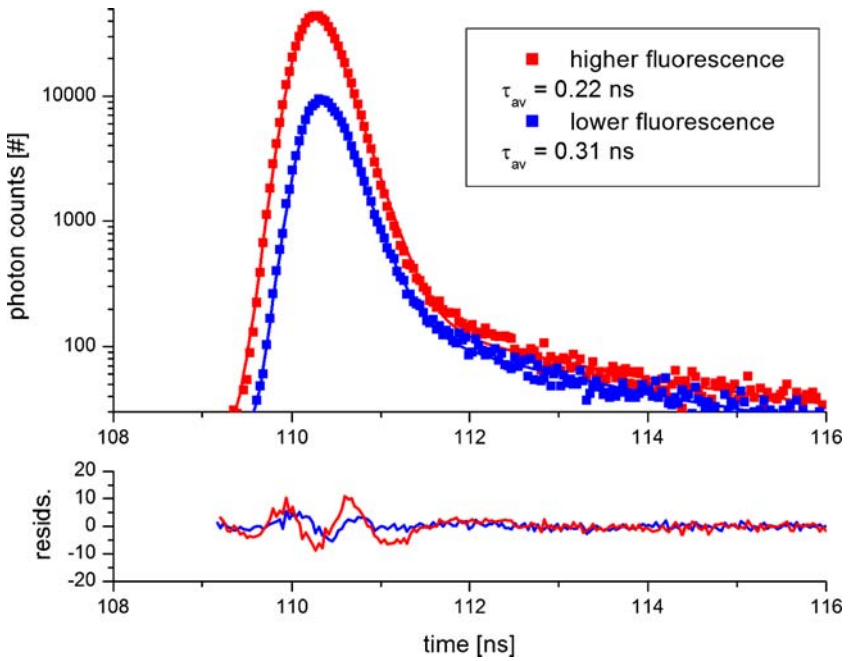

Fig. 10 Fluorescence decays from a 60 nm size metal nanoparticle at higher (*red dots*) and lower (*blue dots*) emission rate. *Solid lines* represent two exponential decay fits with values shown in Table 1. Residual distributions are presented at the bottom graph

of free electrons [27]. These metal clusters are made mostly from gold and silver via different methods [28–30] and have high quantum efficiency values up to 0.41 [31]. In addition, multiphoton absorption-induced luminescence in these nanoclusters has also been observed [32, 33]. Fluorescence has also been observed in silver oxide layers [34, 35]. It is believed that small metal clusters are formed in these layers by photo-irradiation and that the fluorescence originates from these metal clusters.

In the case of metal nanoparticles which are larger then a few nanometers, the origin of the fluorescence is unclear. The localised surface plasmon resonance, typical for these NPs, is not causing fluorescence; the coherent electron motion is non-radiatively de-excited in the order of femtoseconds [36]. Nevertheless, some authors observed dependence of the fluorescence on LSPR [37–39]. They explain the fluorescence by intraband electron hole transitions as in the case of bulk metal, but the LSPR increases the local excitation field and therefore electron-hole generation. The observed fluorescence is several orders higher than from bulk metal but still much lower than fluorescence from metal clusters.

Our emission spectra are similar to those found in the literature [35], where fluorescence was emitted from metal nanoclusters formed in silver oxide layers. It was also reported [40] that by exposing small silver NPs to oxygen, fluorescence from the NPs was observed. Geddes et al [23] observed blinking behaviour for a range of silver structures, for example, fractal-like surfaces and silver island film surfaces, where the detailed behaviour was dependent on the type of structure and on the irradiance. We believe that the fluorescence from our patterned NPs is caused by silver atom clusters which are created in the oxidised outer layer of the metal NPs. The multipeaked spectra are probably caused by formation of clusters with different numbers of atoms, causing a shift in emission [27].

Substrates with metallic nanostructures are currently being tested for the enhancement of Raman and fluorescence signals [7, 12, 41, 42]. For applications in biosensing, not only is signal enhancement important, but so also is the suppression of background noise [43]. A combination of both of these factors leads to improved limit of detection and sensitivity. Clearly, the fluorescence and blinking behaviour of the NPs which is reported here, could impact negatively on efforts to produce improved biosensing via plasmonic enhancement. However, arising from this study, we propose some corrective strategies which should minimise the fluorescent background effect and hence enable the achievement of the full potential of plasmonic enhancement. Investigations are ongoing in our laboratory to introduce a non-permeable coating on the NPs which will eliminate the cluster growth by excluding oxygen from the NP surface. It is also possible to select fluorescent labels which have an appropriate excitation wavelength outside of the NP excitation region i.e. at wavelengths >500 nm.

Conclusion

In conclusion, a simple and reproducible method for μ-patterning substrates with metal nanoparticles was presented. This method is very versatile, allowing creation of metallic nanostructures with different plasmonic properties on planar substrates for application in plasmon-enhanced optical biochips. Substrates with two types of silver nanoparticles were patterned and their optical properties were investigated. We observed an intrinsic fluorescence and blinking behaviour from the NPs which is not related to the plasmonic properties. We have ascribed this fluorescence to the formation of small clusters of metal atoms on the NP surface under oxidative conditions. In order to minimise this background contribution to plasmonic enhancement of fluorescent labels, it is proposed to add a non-permeable outer layer to the NPs. An alternative strategy would be to select a fluorescent molecule whose absorption band does not coincide with the excitation properties of the metal NPs.

References

1. Dragoman M, Dragoman D (2008) Plasmonics: applications to nanoscale tetrahertz and optical devices. Prog Quantum Electron 32:1–41
2. Kreibig U, Vollmer M (1995) Optical properties of metal clusters. Springer series in material science. Springer-Verlag, Berlin Heidelberg
3. Hutter E, Fendler JH (2004) Exploitation of localized surface plasmon resonance. Adv Mater 16:16851706
4. Wilson R (2008) The use of gold nanoparticles in diagnostics and detection. Chem Soc Rev 37:2028
5. Biju V, Itoh A, Sujith A, Ishikawa M (2008) Semiconductor quantum dots and metal nanoparticles: synthesis, optical properties, and biological applications. Anal Bioanal Chem 391:2469
6. Rosi NL, Mirkin CA (2005) Nanostructures in biodiagnostics. Chem Rev 105:1547–1562
7. Green M, Liu FM, Cohen L, Kollensperger P, Cass T (2006) SERS platforms for high density DNA arrays. Faraday Discuss 132:269–280
8. Ditlbacher H, Fedlidj N, Krenn JR, Lamprecht B, Leitner A, Aussenegg FR (2001) Electromagnetic interaction of fluorophores with designed two-dimensional silver nanoparticle arrays. Appl Phys B Laser Optic 73:373–377
9. Ihara M, Tanaka K, Sakaki K, Honma I, Yamada K (1997) Enhancement of the absorption coefficient of cis-(NCS)2 Bis(2, 2′-bipyridyl-4, 4′-dicarboxylate) ruthenium (II) dye-sentisized solar cells by a silver island film. J Phys Chem B 101:5153–5157
10. Stuart HR, Hall DG (1996) Absorption enhanced in silicon on-insulator waveguides using metal island films. Appl Phys Lett 69 (16):2327–2329

11. Rivas L, Sanchez-Cortes S, Garcia-Ramos JV, Morcillo G (2001) Growth of silver colloidal particles obtained by citrate reduction to increase the raman enhancement factor. Langmuir 17:574–577
12. Stranik O, McEvoy HM, McDonagh C, MacCraith BD (2005) Plasmonic enhancement of fluorescence for sensor applications. Sens Actuators B 107(1):148–153
13. Yoshinobu T, Suzuki J, Kurooka H, Moon WC, Iwasaki H (2003) AFM fabrication of oxide patterns and immobilization of biomolecules on Si surface. Electrochim Acta 48:3131
14. Sondag-Huethorst J, Van Helleputte HRJ, Fokkink LJG (1994) Generation of electrochemically deposited metal patterns by means of electron bean (nano) lithography of self-assembled monolayer resists. Appl Phys Lett 64:285
15. Nooney R, Stranik O, McDonagh C, MacCraith BD (2008) Optimisation of plasmonic enhancement of plastic substrates. Langmuire 24(19):11261–11267
16. Schonhoff M (2003) Self-assembled polyelectrolyte multilayers. Curr Opin Colloid Interface Sci 8:86–98
17. Hammond PT (2004) Form and function in multilayer assembly: new application at the nanoscale. Adv Mater 16:1271–1293
18. Kidambi S, Chan C, Lee IS (2004) Selective deposition on polyelectrolyte multilayers: self-assembled monolayers of m-dPEG acid as molecular template. J Am Chem Soc 126:4697
19. Berg MC, Choi J, Hammond PT, Rubner MF (2003) Tailored micropatterns through weak polyelectrolyte stamping. Langmuir 19:2231
20. Tan YW, Dai XH, Li YF, Zhu DB (2003) Preparation of gold, platinum, palladium and silver nanoparticles by the reduction of their salts with a weak reductant-potassium bitartrate. J Mater Chem 13:1069–1075
21. Jiang X (2002) Polymer-on-polymer stamping: universal approaches to chemically patterned surfaces. Langmuir 18:2607
22. Mie G (1908) Beitrage zur Optik trueber Medien speziell kolloidaler Mettalloesungen. Ann Phys 25:377–445
23. Geddes CD, Parfenov A, Lakowicz JR (2003) Luminescent blinking from noble-metal nanoclusters: new probes for localization and imaging. J Fluoresc 113(4):297–299
24. Lakowicz JR (1999) Principles of fluorescence spectroscopy, 2nd edn. Kluwer Academic/Plenum, New York
25. Mooradia A (1969) Photoluminescence of metals. Phys Rev Lett 22(5):185
26. Boyd G, Yu ZH, Shen YR (1986) Photoinduced luminescence from the noble metals and its enhancement on roughened surfaces. Phys Rev B 33(12):7923
27. Zheng J, Nicovich PR, Dickson RM (2003) Highly fluorescent noble-metal quantum dots. Annual Rev Phys Chem 58:409
28. Felix C, Sieber C, Harbich W, Buttet J, Rabin I, Schulze W, Ertl G (2001) Ag8 fluorescence in argon. Phys Rev Lett 86(14):2992
29. Shang L, Dong SJ (2008) Facile preparation of water-soluble fluorescent silver nanoclusters using a polyelectrolyte template. Chem Commun 9:1088
30. Zheng J, Dickson RM (2002) Individual water-soluble dendrimer-encapsulated silver nanodot fluorescence. J Am Chem Soc 124:13982
31. Zheng J, Petty JT, Dickson RM (2003) High quantum yield blue emission from water soluble Au8 nanodots. J Am Chem Soc 125: 7780–7781
32. Kempa T, Farrer RA, Giersig M, Fourkas JT (2006) Photochemical synthesis and multiphoton luminescence of monodisperse silver nanocrystals. Plasmoncs 1:45–51
33. Farrer R, Butterfield FL, Chen VW, Fourkas JT (2005) Highly efficient multiphoton-absorption-induced luminescence from gold nanoparticles. Nano Lett 5(6):1139
34. Peyser LA, Vinson AE, Bartko AP, Dickson RM (2001) Photoactivated fluorescence from individual silver nanoclusters. Science 291(5501):103–106
35. Mihalcea C, Buchel D, Atoda N, Tominaga J (2001) Intrinsic fluorescence and quenching effects in photoactivated reactively sputtered silver oxide layers. J Am Chem Soc 123:7172
36. Link S, El-Sayed MA (1999) Spectral properties and relaxation dynamics of surface plasmon electronic oscillations in gold and silver nanodots and nanorods. J Phys Chem B 103(40):8410–8426
37. Mohamed MB, Volkov V, Link S, El-Sayed MA (2000) The "lightening" gold nanorods: fluorescence enhancement of over a million compared to the gold metal. Chem Phys Lett 317(6):517–523
38. Zhu J, Zhu X, Wang YC (2005) Electrochemical synthesis and fluorescence spectrum properties of silver nanospheres. Microelectron Eng 77:58–62
39. Lereu A, Sanchez-Mosteiro G, Ghenuche P, Quidant R, van Hulst NF (2008) Individual gold dimers investigated by far- and near-field imaging. J Microsc-Oxford 229(2):254
40. Balan L, Malval JP, Scneider R, Burget D (2007) Silver nanoparticles: new synthesis, characterization and photophysical properties. Mater Chem Phys 104:417
41. Geddes CD, Cao H, Gryczynski Z, Fang JY, Lakowicz JR (2003) Metal-Enhanced fluorescence (MEF) due to silver colloids on a planar surface: potential application of indocyanime green to in vivo imaging. J Phys Chem A 107:3443–3449
42. Mayer C, Schalkhammer T (2003) Robust nano cluster layers for structural amplified fluorescence biochips. Rev Adv Mater Sci 5:53–56
43. Rabbany SY, Donner BL, Ligler FS (1994) Optical immunosensors. Crit Rev Biomed Eng 22:307–346